OBSERVATIONS AND RESTRICTIONS FOR TRACKING INDICES MEASUREMENT IN MATERIALS TESTING

A. Fuchs and H. Zangl

Graz University of Technology

Institute of Electrical Measurement and Measurement Signal Processing

Kopernikusgasse 24, 8010 Graz, Austria

Email: anton.fuchs@tugraz.at

Abstract- The testing of various carrier materials for circuit paths on the basis of tracking indices determination is of particular interest for many modern sensing technologies, especially for technologies based on capacitive methods, as well as for the protection of circuitries by means of sealing in insulator material. This paper discusses observations for the determination of the tracking indices for elastic insulators according to the DIN standard EN 60112. The appearance of burn-in patterns on the insulator surface and the peculiar decrease of current peak amplitudes with increasing number of electrolyte droplets are investigated and possible causes are discussed, based on Finite Element Analysis and camera images of conducted experiments.

Index terms*: tracking indices, leakage current, elastic insulating material, DIN EN 60112

I.   INTRODUCTION

Tracking in conjunction with testing of insulating material means the irreversible degradation of surface material from the formation of conductive carbonized paths [1]. For many modern sensing technologies the insulating carrier material, on which electrode structures and circuit paths are placed, has crucial importance for life expectancy and reliability of sensor products. To hinder reverse engineering or to make electric circuits and devices shock- or waterproof, circuitries may be sealed in insulating materials like composition rubber. The determination of the tracking indices of solid insulating material is then of importance for certain industrial applications as well as for research activities and characterization and classification in materials

science [2]. The insulating material is exposed to electrical and chemical (electrolytical) stress, causing the above mentioned carbonized paths on the surface or in the material.

For example, the pollution layer of wet or dry type has an enhancement effect on the distribution of the electric potential, field and leakage current on the surface of high-voltage outdoor insulators [3-6]. Transformers, which are built with tight insulation tolerances, are subject to various aging stresses. While the aging of the insulation material becomes gradually more severe, the leakage current generally tends to increase and arcing discharge may occur [7].

The proof tracking indices (PTI values of insulators) of the different solid materials are employed as acceptance criterion as well as a measure for quality inspection of materials and formed parts. The test procedure for the PTI value of the material comprises to insert 50 droplets of an electrolytic solution subsequently on the material surface between two electrodes with a certain alternating voltage. The PTI value in V (withstand voltage) indicates the maximum tested inter-electrode voltage that did not cause tracking failure (i.e. no formation of conductive paths and hence no current exceeds 500 mA for more than 2 s) during the impact of the 50 droplets. The comparative tracking indices (CTI values of insulators) are mainly used for the basic characterization and comparison of material properties and are described in a DIN standard as well [8].

For the determination of the tracking indices, two electrodes – one with a high voltage AC signal and the other on ground – are placed on the insulator surface [8, 9]. For both measures, an aqueous solution of Ammonium Chloride is applied drop by drop on the surface in-between the two electrodes to contaminate and hence "artificially" age the material by means of electrical and chemical (electrolytic) impact.

Numerous attempts have been undertaken to model contaminated (polluted) surfaces of solid insulators [10, 11] and various embodiments to determine the degree of pollution on the basis of leakage current measurement are known [7, 9, 12].

This paper discusses additional observations and restrictions for the determination of the tracking indices of elastic, rather soft, solid insulating materials. The testing procedure for tracking indices in the valid standard is investigated by means of evaluating current signals, video images, and Finite Element Analysis (FEA).

II.   MEASUREMENT SETUP

According to the DIN standard for the determination of the proof and comparative tracking indices of solid insulating material [8], a measurement setup with two chisel-shaped electrodes was designed. Figure 1 shows the principle structure of this setup, which also comprises an adjustable, non-conducting frame that holds the PVC electrode support, and a syringe for well-defined droplet insertion. A scale and weights are used in order to ensure constant force of the electrodes onto the test specimen as suggested in the standard. One electrode is connected to a 400 V AC signal with 50 Hz and the current between the active electrode and the grounded one is determined by means of voltage measurement on a resistor. When a droplet of the electrolytic solution hits the surface of the insulator material under test, the inter-electrode resistance decreases significantly and the resulting current heats up the fluid film between the electrodes causing evaporation of parts of the fluid media.

The gap between the electrodes on the material surface is 4 mm and the chisel-shaped electrodes are pressed onto the material with 1 N as demanded by the standard.

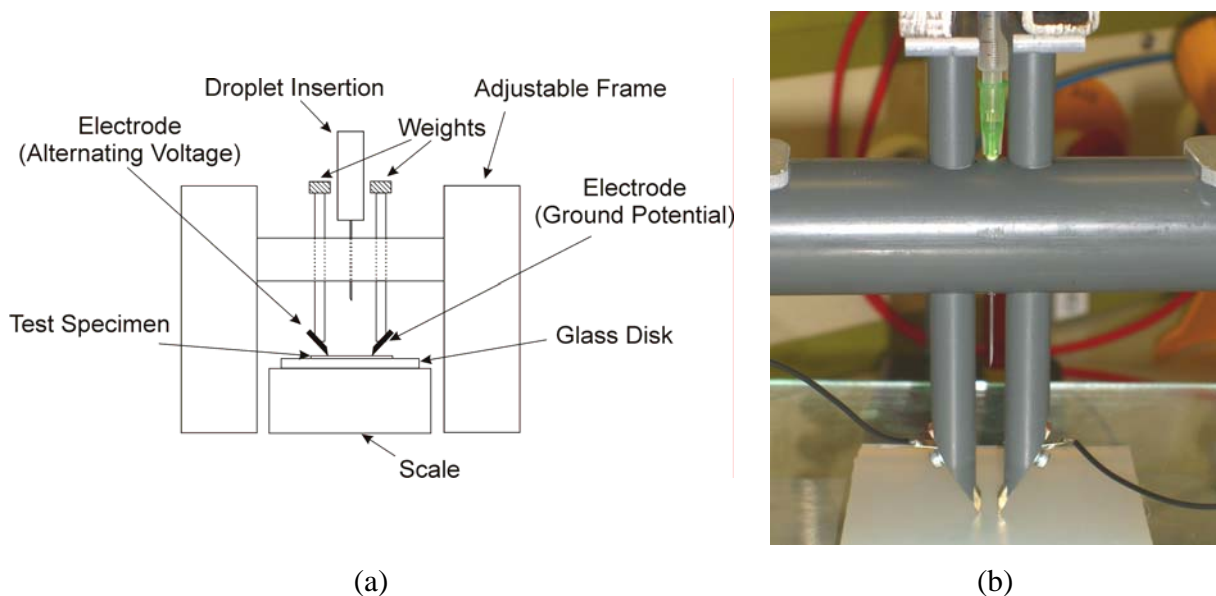(a)   (b)

Figure 1. (a): Sketch of the measurement setup comprising electrodes on a support device and droplet insertion and (b) Photo of the measurement setup with the PVC support frame, the syringe, and the electrodes [2].

The electrodes have not been made of Platinum with purity of at least 99 % as suggested in the standard [8], but of aureate copper. This choice of material is more realistic to be found in electronic circuits than the inert Platinum.

An amount of 0.1 mass per cent Ammonium Chloride (NH_4Cl) is dissolved in distilled water, so that the solution has a specific conductivity of 4 Ωm. Every 30 seconds a droplet of this solution is inserted on the material surface by means of the syringe. A total number of 50 droplets is used for one full test cycle (i.e. for one specific voltage) and the experiment is aborted when the current between the electrodes exceeds 500 mA or when a permanent flame on the relevant surface section can be observed. The material is then not approved for the PTI value of tested voltage.

The measurement results for the determination of the tracking indices for rubber-like insulation materials reveal two noticeable problems that will be discussed in this paper – the burn-in of a pattern in-between the two electrodes and a decrease of signal amplitudes with increasing number of solution droplets.

III.   BURN-IN PATTERNS

The first observed phenomenon during testing of rubber-like materials was the burn-in of certain patterns in the middle of the two electrodes. For test voltages below 300 V the current density is not sufficient to cause a burn-in pattern in the insulator surface, for test voltages of 400 V and higher, burn-in patterns are manifest. Deep and significant patterns occur after 20 to 30 droplets latest and represent a change in the surface structure of the material under test. Figure 2 shows a sequence of high-speed camera images for the measurement setup in Figure 1. At the time step t=0 ms a droplet has hit the insulator surface and the electrolytic fluid connects the two electrodes. The current between the electrodes heats up the fluid and causes evaporation. At the time step t=376 ms the first sparks in the middle of the electrodes can be observed in the digital images. It is important to note that in all experiments sparks always occurred in parallel to the electrodes' surfaces and not from one electrode to the other. Depending on the test voltage the sparks remain for more than a second and are of high intensity.
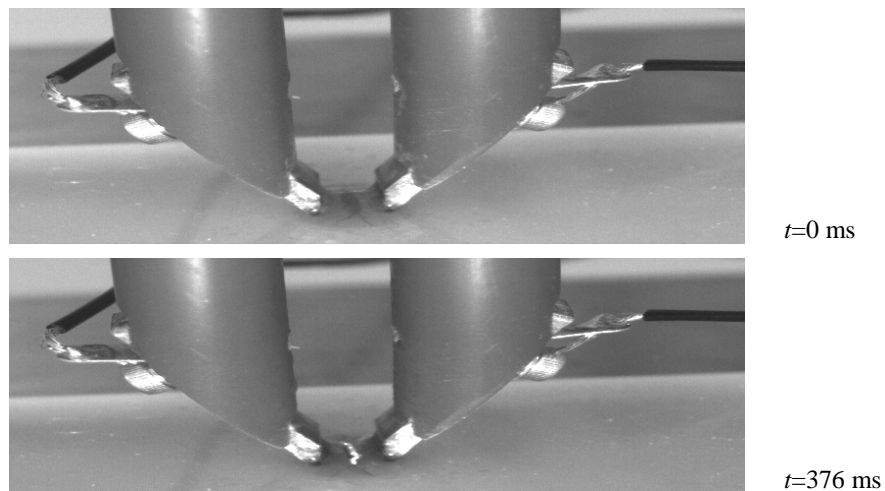
t=0 ms

t=376 ms

Figure 2. Photo of the relevant insulator surface when the droplet hits the material (*t*=0 ms) and when the first sparks can be observed in the images (*t*=376 ms).

The burn-in pattern is significant and well-developed. Figure 3 shows a photo of this pattern. The black vertical lines in the figure mark the contact lines of the electrodes with the elastic test specimen. It can be seen in both the camera images and the burn-in pattern that the sparks occur locally in the middle of the electrodes also causing flashovers beyond the length of the electrodes.
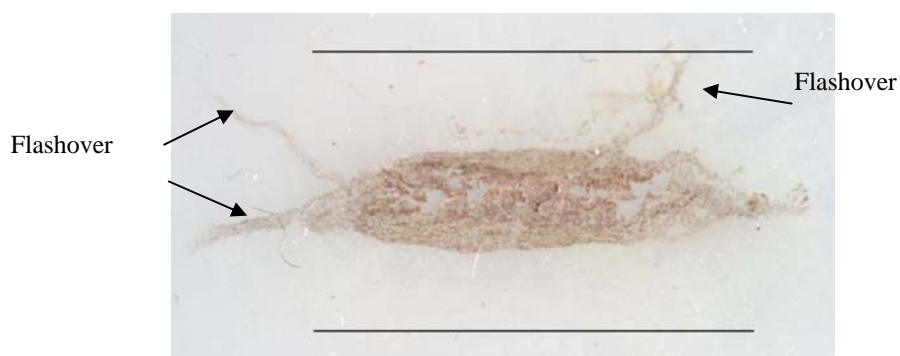

Figure 3. Photo of a burn-in pattern as a result of PTI testing at a voltage of 400 V using the setup in Figure 1; Distance between the electrodes (black lines) is 4 mm.

On closer examination, the weights with which the electrodes are pressed against the test specimen seemed to be the reason for this local pattern. Due to the mechanical stress caused by the chisel-shaped electrodes, the elastic material is deformed so that the contact lines under the electrodes show the highest and the section in the middle of the electrodes exhibit the lowest

deformation. Consequently, when a thin film of conducting fluid is placed on this surface by means of a droplet, current maxima and hence a thermal hot spot will be found in this center section.

Two materials of different elasticity have been examined - the deformation due to the impact of the chisel-electrodes was 1.210 mm for the softer material and 0.830 mm for the harder material. To estimate the impact of this deformed geometry, FEA is applied to solve the conductive media problem, as shown in Figure 4. When the current density is plotted over the test specimen length between the electrodes (i.e. arc-length positions 0.006 to 0.012), simulation results as shown in Figure 5 can be obtained for the current density. The maximum current density is 1.827e4 A/m^2 for the ideal (non-deformed) case while the current density reaches a value of 2.849e4 A/m^2 for the deformed case, which is an increase of 55.94 %.
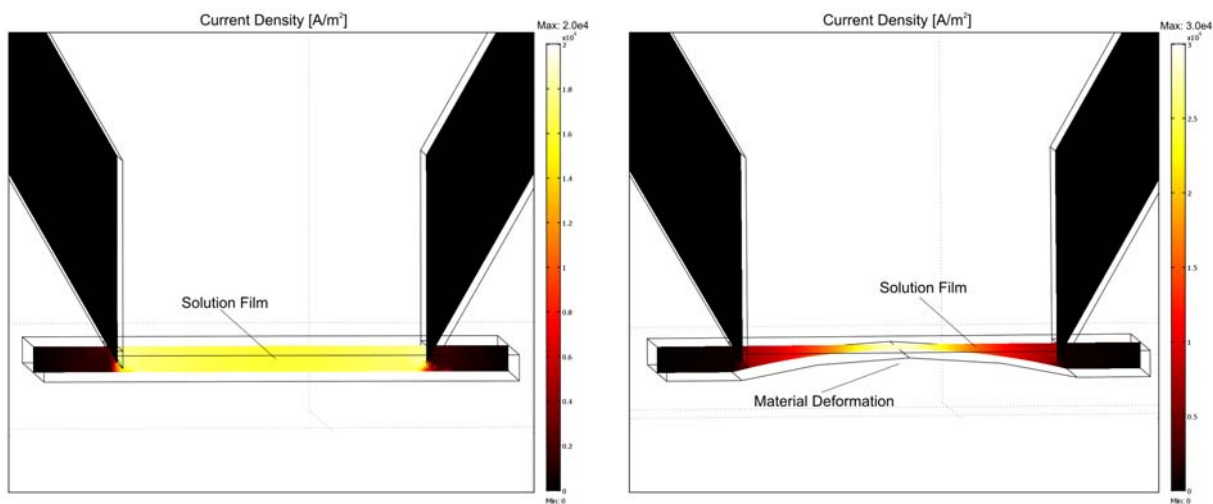

Figure 4. FEA model for the determination of the current density in the solution film (σ=0.25 S/m); (left): Without deformation and (right): With deformation of material below [2].

Camera images reveal that additional to the deformation effects adhesion between the droplet boundary layer and the electrode surface is present. Since the position, where the droplet hits the surface, and also the behavior of the solution while boiling may vary slightly for each droplet, the effect of adhesion can not be described and reliably predicted at this stage.
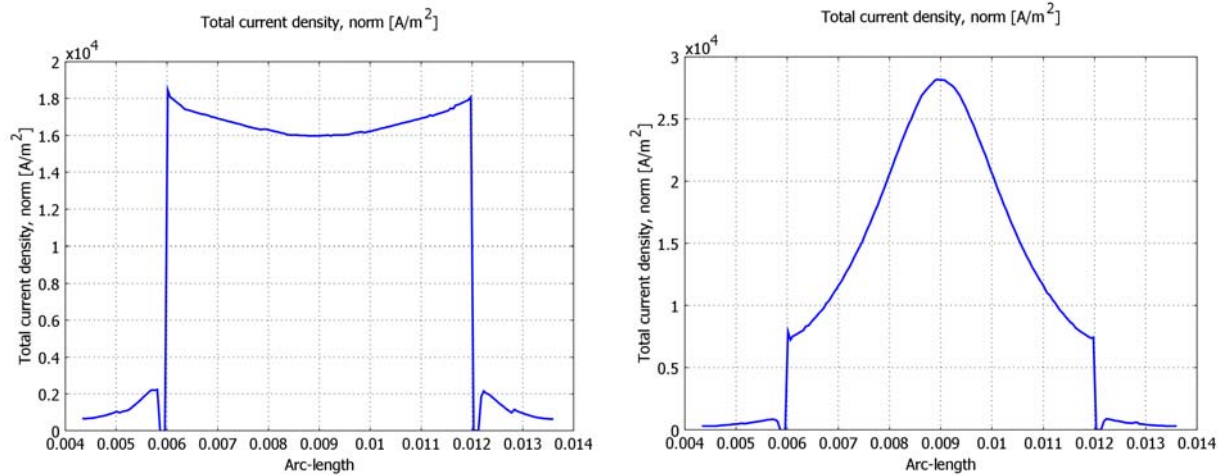
Figure 5. Simulation results for the current density between the electrodes for (left): Non-deformed geometry and (right): Deformed geometry with "hot-spot" in the middle [2].

Figure 6 illustrates the effects of deformation and adhesion for the chisel-shaped electrodes that cause a narrow, significant burn-in pattern.
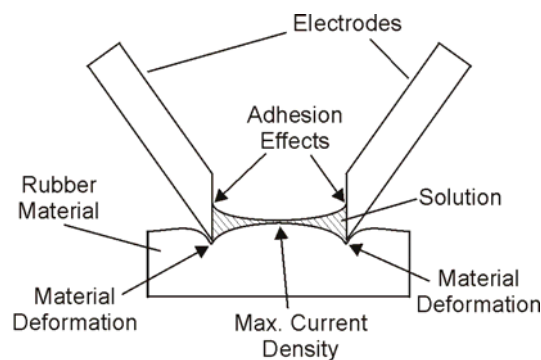

Figure 6. Adhesion and material deformation for chisel-shaped electrodes causing a current density maximum in the middle of the electrodes.

IV.   ALTERNATIVE ELECTRODE STRUCTURES AND ARRANGEMENTS

An arrangement of electrodes as given in Figure 1 is not realistic for most sensor applications. Both material deformation and adhesion effects have an impact on the current density distribution between the electrodes and may consequently falsify results in testing of tracking indices. Two

other electrode arrangements, that are both more likely to be found in practical applications in electrical engineering, have hence been investigated:

a. Chisel-Shaped Electrodes Along the Material Surface

The electrodes used in Section III have been placed flat on the surface of the elastic insulator material so that again a 4 mm gap between the electrodes' tips remains. No additional weights are used for these experiments and material deformation can hence be neglected. The same testing procedure with a test voltage of 400 V and an insertion of the electrolytic fluid onto the surface between the electrodes in drops has been executed.

Figure 7 shows high-speed camera images for the moment a droplet hits the surface and connects the two electrodes via a fluid film (t=0 ms) and the first occurrence of sparks (t=376 ms). In the camera images adhesion effects can be observed again, although the effects seem to be less significant due to the sloped front face of the electrodes. Also for this arrangement the sparks develop at the liquid layer or the boundary layer of the fluid, where the highest current density can be found due to the adhesion of the electrolyte. The sparks show less intensity and no flashovers beyond the length of electrodes could be observed. The burn-in pattern on the insulator surface is shown in Figure 8 – the electrode edges are marked with black lines in this figure.
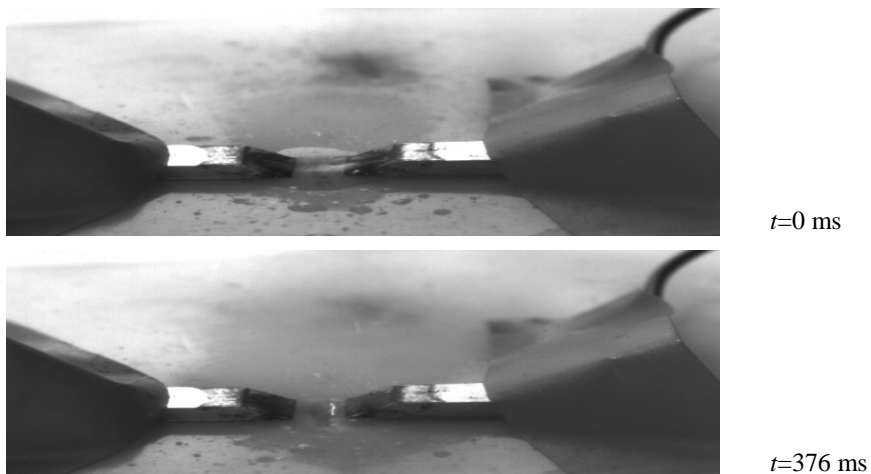

t=0 ms

t=376 ms

Figure 7. Photo of the relevant insulator surface for horizontal chisel-shaped electrodes when the droplet hits the material (t=0 ms) and when the first sparks can be observed (t=376 ms).

Figure 8. Photo of the burn-in pattern as a result of PTI testing at a voltage of 400 V using horizontal chisel-shaped electrodes; Distance between the electrodes (black lines) is 4 mm.

Figure 9 illustrates the effects of adhesion for the chisel-shaped electrodes causing a narrow burn-in pattern that is less significant compared to patterns presented in Section III. Deformation of the material can be neglected since no weights on the electrodes are used in these experiments and the contact surface on the elastic insulator is much higher.
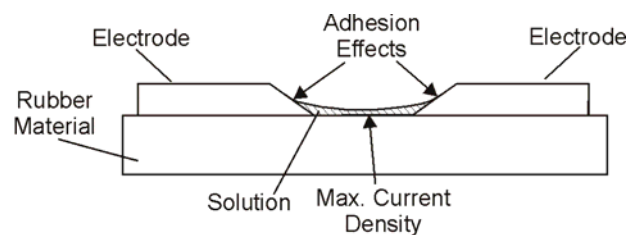

Figure 9. Adhesion effects for horizontal chisel-shaped electrodes causing a current density maximum in the middle of the electrodes.

b. Thin Electrodes along the Material Surface

In modern sensing technologies many applications with flat electrode structures of a few μm to less than a millimeter can be found on various carrier materials. A prominent application, where flat electrode structures can be found is capacitive sensing [13].

To analyze the effect of thin electrode structures on the tracking behavior of a setup, electrodes with a thickness of 0.2 mm have been mounted on the surface of the insulating elastic carrier material. A gap of 4 mm has been left between the two electrodes, of which again one was

excited with a 400 V 50 Hz AC signal while the potential of the second electrode was kept on ground. With this setup both deformation of the material and fluid adhesion on the surface of the electrodes can be mostly neglected. Camera images reveal that a droplet, which hits the surface of the insulator, forms a fluid layer of nearly constant thickness. When the electrolyte starts to evaporate as a result of the electric current, the fluid boundary layer is randomly distributed between the electrodes, also causing randomly distributed sparks, which are roughly in parallel to the electrode edges. The burn-in patterns are hence distributed over the entire gap between the electrodes. A band of weak sparks can be observed in camera images, such as shown in Figure 10, which slowly moves from one electrode to the other while the fluid is evaporating. Figure 11 shows a photo of the resulting burn-in pattern, which differs from the previous ones since it is less intensive and spreads from the edge of one electrode to the other.
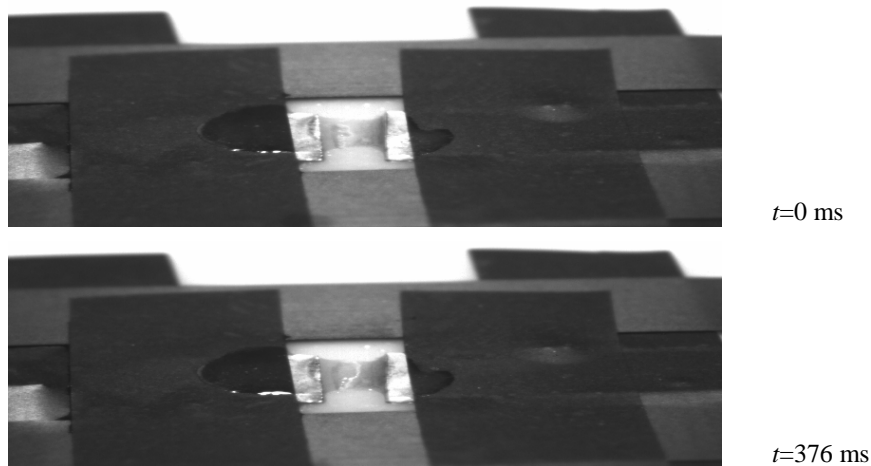

t=0 ms

t=376 ms

Figure 10. Photo of the relevant insulator surface for horizontal flat electrodes when the droplet hits the material (t=0 ms) and when the first spark can be observed in the images (t=376 ms).

Figure 12 depicts the conditions for the use of thin horizontal electrodes: Since material deformation and adhesion can be neglected, the fluid film is of approximately the same thickness. As a result, no significant current density maxima will be found and the occurrence of sparks and consequently the formation of burn-in patterns are randomly distributed.

Figure 11. Photo of the burn-in pattern as a result of PTI testing at a voltage of 400 V using thin horizontal electrodes; Distance between the electrodes (black lines) is 4 mm.
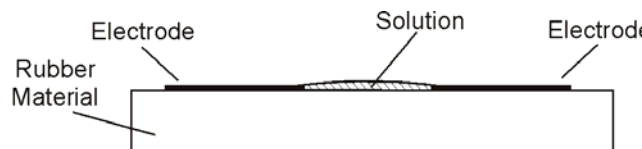

Figure 12. The lack of material deformation and adhesion for horizontal thin electrodes causes no significant current density maxima in-between the electrodes.

V.   IMPACT OF DROPLET EVAPORATION

For all realized electrode structures two types of droplet evaporation could be observed after the electrolyte has hit the surface. In both cases the conductive fluid droplet connects the two electrodes and the resulting current immediately heats up the fluid in-between and causes boiling. For the first type of evaporation, the droplet forms a consistent fluid layer between the electrodes and sparks occur where this layer is thinnest until the film is disconnected. The current signal is measured as the voltage drop on a 50 Ω resistor and is shown in Figure 13a for this smooth type of evaporation. The maximum peak to peak current is about 280 mA in this figure.

In a second type of droplet evaporation, which could also be observed in experiments with all electrode structures, boiling of the fluid causes parts of the droplet to splash onto farther sections of the insulator material. The fluid film is then nearly disconnected and a stepwise delayed firing occurs as a consequence of the eruptive boiling. The voltage drop on a 50 Ω resistor of such an

eruptive evaporation with multiple firing is given in Figure 13b. The maximum peak to peak current is about 360 mA in this figure.
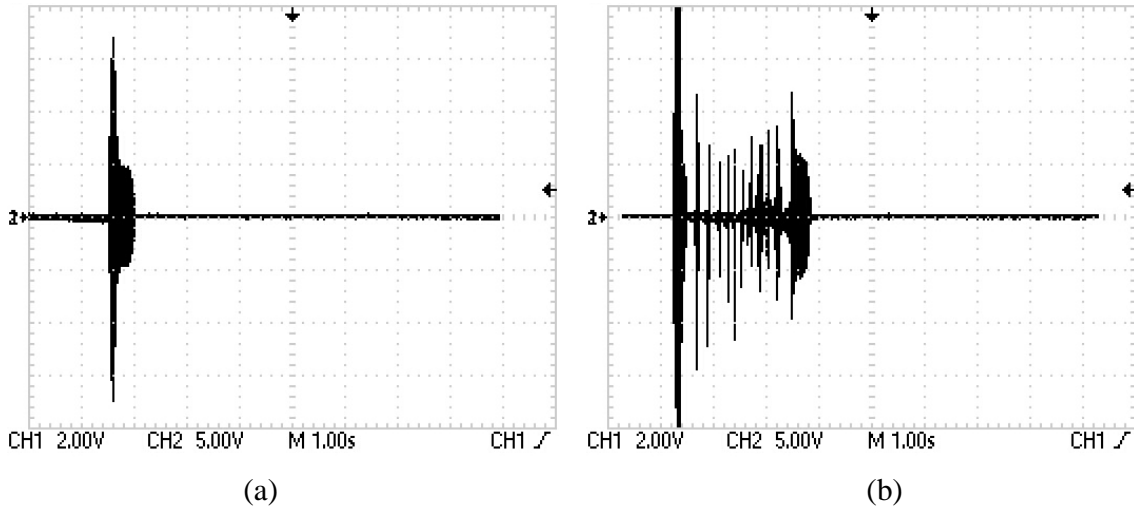

Figure 13. Voltage drop on a 50 Ω resistor for (a): Smooth evaporation and (b): Eruptive evaporation of a droplet on the surface of the insulator material.

The detail plot of the current signal on a 50 Ω resistor in Figure 14 shows the non-linear, time variant characteristic of the resistance that is formed by the fluid layer in-between the electrodes.
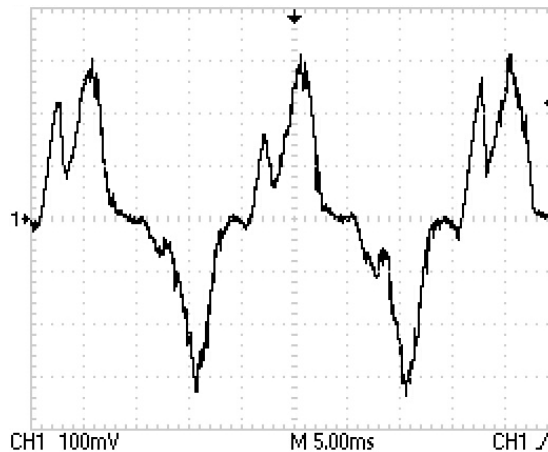

Figure 14. Detail plot of the current proportional voltage drop on a 50 Ω resistor.

VI.   DECREASING CURRENT AMPLITUDES

The second observed phenomenon while testing the insulator material on tracking behavior is the decrease of current peak amplitude with increasing number of added droplets. The electric current between the electrodes evaporates the distilled water in the solution film and causes reduced resistivity when drying. As a consequence, the peak signal amplitudes fade away with time, as can also be seen in Figure 13. Figure 15 shows a diagram representing the signal power trend in recorded current signals for an increasing number of droplets. It can be observed that especially for the first couple of droplets the amplitude levels decrease too, although more ions should become available on the surface.

During the experiments with the 400 V test voltage, an interaction of the solution droplets with the aureate copper electrodes could be observed. A thin greenish layer – most likely Copper(I) Chloride (CuCl) – covers parts of the electrodes after a few droplets have hit the surface of the test specimen.
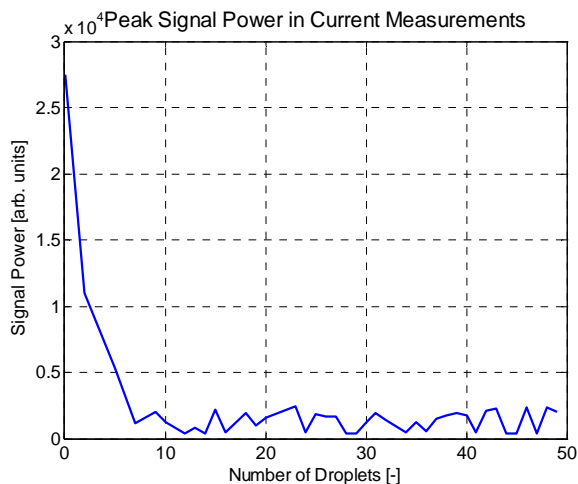
Figure 15. Signal power of the current measurement results vs. number of droplets [2].

It is known that metals that are not inert may show some interaction with both the used electrolytes and the insulation material. For the conducted experiments, it is most likely that the contamination of the electrode surfaces due to electrical and chemical stresses increases the contact resistances for the transitions between electrode head and the test specimen. This can be caused by a CuCl coating itself or by the altered moistening behavior due to the contamination of the electrode and insulation material.

Finite Element Method simulations have been conducted to obtain an estimation of the influence of increased contact resistance on the current distribution between the electrodes. A thin layer that represents the transition section between electrodes and test specimen is set to a different material conductivity (1.8e-13 S/m) to simulate weak conducting CuCl coating. Simulation results reveal that the maximum current density without the electrode coating is 365.3 A/m^2 while it is only 133.9 A/m^2 with the weak conducting layer, which corresponds to a decrease of signal amplitude of 63.35 %.

VII.   CONCLUSION

This paper discusses observations and findings for the determination of the tracking indices of elastic insulating materials that have occurred during measurements according to the standard DIN EN 60112. Two substantial observations have been made, namely the appearance of burn-in patterns on the insulator surface and the peculiar decrease of current peak amplitudes with increasing number of electrolyte droplets.

The burn-in patterns are the result of current density maxima that can be found in-between the electrodes. Significant hot spots are caused by the deformed geometry of the elastic media due to the chisel-shaped electrodes and by adhesion. Burn-in patterns are less significant when material deformation is avoided and weakest patterns and hence least variation of the insulator surface can be achieved when thin, flat electrodes are utilized for testing.

The decreasing current amplitudes are most likely the result of increasing contact resistance (interaction of the electrode with the electrolyte).

REFERENCES

[1].   -, "Authoritative Dictionary of IEEE Standards Terms", Seventh Edition, IEEE Press, 2000.

[2].   A. Fuchs and H. Zangl, "Observations and Findings for the Determination of the Tracking Indices of Elastic Insulating Materials", Proc. of the 2nd International Conference on Sensing Technology, Palmerston North, New Zealand, pp. 265-269, Nov. 26-28, 2007.

[3].   A. Ahmed, H. Singer, P. Mukherjee, "A numerical model using surface charges for the calculation of electric fields and leakage currents on polluted insulator surfaces", Proc. of

the Conference on Electrical Insulation and Dielectric Phenomena, Vol. 1, pp. 116–119, Oct. 25-28, 1998.

[4]. P. Mukherjee, A. Ahmed, H. Singer, "Electric field distortion caused by asymmetric pollution on insulator surfaces", IEEE Transactions on Dielectrics and Electrical Insulation, Vol. 6, No. 2, 1999, pp. 175–180.

[5]. G. Gerdin, V. Lakdawala, P. Basappa, "Computation of ac and dc electric field around a wet polluted insulator", Proc. of the Conference on Electrical Insulation and Dielectric Phenomena, pp. 176-179, Oct. 20-24, 2002.

[6]. P. Basappa, M. Williams, K. Agarwal, "Computation of electrostatic field around a partially wet insulator surface through numerical techniques and simulation", Conference Record of the 2004 IEEE International Symposium on Electrical Insulation, pp. 292-295.

[7]. M. Mousavi, K. Butler-Purry, "Experimental investigation of distribution transformer aged solid insulation", Proc. of the 45th Midwest Symposium on Circuits and Systems, Vol. 2, pp. 192-195, Aug. 4-7, 2002.

[8]. -, "Method for the determination of the proof and the comparative tracking indices of solid insulating materials", Standard: DIN EN60112, Classification VDE0303, Part 11, Nov. 2003.

[9]. F. Youssef, T. Eish, "Effect of electrode coating on leakage current and surface flashover strength in polymers", Proc. of the 6th International Symposium on Electrets, pp. 344-348, Sep. 1-3, 1988.

[10]. H. Woodson, A. Mcelroy, "Insulators with Contaminated Surfaces, Part III: Modeling of Dry Zone Formation", IEEE Transactions on Power Apparatus and Systems, Vol. PAS-89, Nr. 8, 1970, pp. 1868-1876.

[11]. A. Mekhaldi, D. Namane, S. Bouazabia, A. Beroual, "Empirical model of a high voltage insulator under nonuniform pollution", Proc. of the 11th International Symposium on High Voltage Engineering, Vol. 4, pp. 232-235, Aug. 23-27, 1999.

[12]. H. Matsuo, T. Fujishima, T. Yamashita, "Relation between leakage impedance and equivalent salt deposit density on an insulator under a saltwater spray", IEEE Transactions on Dielectrics and Electrical Insulation, Vol. 6, No. 1, 1999, pp. 117-121.

[13]. L.K. Baxter, "Capacitive Sensors - Design and Application", IEEE Press Series on Electronics Technology, New York, 1997.